Desalination and Water Treatment
www.deswater.com

doi:10.5004/dwt.2019.24147

159 (2019) 290–303
August

Synthesis and characterization of polymer microspheres and its application for phenol adsorption

İnci Özdemir[a], Ali Kara[b,*], Nalan Tekin[c,*], Asım Olgun[b]

[a]*Kocaeli University, Izmit Vocational School, Property Protection and Security Department, 41285, Kocaeli, Turkey, Tel. +905326801742, email: akkaninci@gmail.com (İ. Özdemir)*
[b]*Uludag University, Science and Art Faculty, Department of Chemistry, 16059, Bursa, Turkey, Tel. +902242941733, email: akara@uludag.edu.tr (A. Kara), Tel.. +902242942863, email: asimolgun@uludag.edu.tr (A. Olgun)*
[c]*Kocaeli University, Science and Art Faculty, Department of Chemistry, 41380, Kocaeli, Turkey, Tel. +902623032031, email: nalanisiktekin@gmail.com (N. Tekin)*

Received 3 November 2018; Accepted 20 March 2019

ABSTRACT

This paper reports synthesis of the poly(ethylene glycol dimethacrylate-*n*-vinyl imidazole) (*[poly(EGDMA-VIM)]*) microspheres by suspension polymerization for the removal of phenol from an aqueous solution. The synthesized *[poly(EGDMA-VIM)]* microspheres were characterized by various analysis techniques. The *[poly(EGDMA-VIM)]* microspheres possessed a high specific surface area (304.4 $m^2 g^{-1}$). It was found that the pseudo-second-order kinetic and Freundlich isotherm models could well define the phenol adsorption process. The maximum capacity of the *[poly(EGDMA-VIM)]* microspheres was calculated to be 34.7441 mg g^{-1} at 298 K and natural pH from Langmuir isotherm. The adsorption thermodynamics revealed that the adsorption of phenol was an exothermic and spontaneous process. The *[poly(EGDMA-VIM)]* microspheres were easily regenerated by using a 0.01 M NaOH solution, and were repeatedly used for at least 5 cycles without losing the adsorption capacity. The experimental results suggest that the *[poly(EGDMA-VIM)]*microspheres can be implemented as a promising adsorbent for phenol removal from wastewater.

Keywords: Adsorption; N-vinylimidazole; Ethylene glycol dimethacrylate; Polymer microspheres; Phenol

1. Introduction

Phenol is often used in many industrial processes [1–3] and is a priority hazardous pollutant because of its toxicity even at low concentrations [4]. The utilization of phenol-contaminated water influences the health of the eyes, digestive system, brain, lungs, liver, heart, skin, and kidney [5]. Therefore, the removal of phenol from contaminated water is very important for aquatic life and human health. Various techniques [4,6–12] have been used for the removal of phenol, and adsorption is one of the most frequently used techniques for phenol removal because of its high removal efficiency, simplicity, low operational cost, availability to be used with various adsorbents, and lack of detrimental byproducts in treated water [13]. Several adsorbents [14–21] have been used for the removal of phenol from aqueous solutions, but they have some disadvantages such as, intra-particle resistance, low adsorption, and regeneration of the adsorbent [4]. Therefore, development of novel adsorbents for the removal of phenol from wastewater remains an important challenge.

Recently, porous polymeric adsorbents synthesized for phenol removal have attracted significant attention due to feasible regeneration for repeated use, a perfect skeleton strength, physicochemical properties, and their high surface area [1]. Also, a high adsorption capacity for the removal of phenol and substituted phenols was found in the porous polymeric adsorbents [1,4,22–30]. Among these porous polymeric adsorbents, it is expected that polymer beads have a large adsorption capacity for inorganic/

*Corresponding author.

organic contaminants because of their high surface areas [24]. In our previous studies, we reported the adsorption capacity of the poly(ethylene glycol dimethacrylate-*n*-vinyl imidazole) [poly(EGDMA-VIM)] beads for Cr(VI) [31], Hg(II), Cd(II), and Cu(II) [32] as well as its immobilization of tyrosinase [33], yeast invertase [34], and α-amylase [35] on Cu^{2+} chelated [poly(EGDMA-VIM)] beads. Additionally, the poly(ethylene glycol dimethacrylate-*co*-vinylimidazole) was used for removal of Cd^{2+} [36], and Pb^{2+} [37] as well as the solid phase extraction of selected non-steroidal anti-inflammatory drugs [38] and purification and isolation of phenolic acids [39]. Furthermore, PEGMA-VI microspheres were used as an adsorbent for removal of Cu(II) [40], Cr(VI), and Ni(II) [41].

In this study, the synthesis of cross-linked poly(ethylene glycol dimethacrylate-*n*-vinyl imidazole) *[poly(EGDMA-VIM)]* microspheres synthesized by suspension polymerization from *N*-vinyl imidazole (VIM) and ethylene glycol dimethacrylate (EGDMA) is reported. After the synthesis, the characterization of the polymer microspheres was carried out by various structural, morphological, and thermal analysis methods. In the present study, the surface area of the *[poly(EGDMA-VIM)]* microspheres is higher than that of the beads used in the previous studies [31–35]. The prepared *[poly(EGDMA-VIM)]* microspheres were used as an adsorbent for phenol removal. To our knowledge, the *[poly(EGDMA-VIM)]* microspheres for removal of phenol had never been investigated. The effects of temperature, adsorbent dosage, and initial concentrations of phenol solutions, as well as contact time and pH of solutions on the adsorption process were studied. The adsorption mechanisms for phenol removal onto the *[poly(EGDMA-VIM)]* microspheres were probed using FTIR (Fourier transformation infrared spectroscopy), XPS (X-ray photoelectron-spectroscopy), and XRD (X-ray diffraction) analysis. The equilibrium data of phenol adsorption were analyzed and fitted with isotherm kinetic models. Desorption efficiency of the *[poly(EGDMA-VIM)]* microspheres after phenol adsorption was also interpreted. Furthermore, the polymer microspheres were found to be reusable, which is required for the industrial application of any adsorbent, after 5 instances of desorption of the adsorbed phenol. Due to their ease of synthesis, high surface area, remarkable adsorption capacity, ease of desorption process, and reusability, the *[poly(EGDMA-VIM)]* microspheres can be effectively applied as an alternative for the removal of phenol and various pollutants from wastewater.

2. Materials and method

2.1. Materials

PVAL, Poly(vinyl alcohol) (98% hydrolyzed, M_w: 100.000), and VIM, *N*-Vinyl imidazole were obtained from Aldrich (Steinheim, Germany). *VIM* was used as an organic functional monomer after distillation at 74 to 76°C and 10 mm Hg. EGDMA, ethylene glycol dimethacrylate (≤98.0%),was purchased from Merck (Darmstadt, Germany) and used as a cross-linking agent after purification with active alumina and then stored at 4°C. AIBN, 2,2′-Azobisisobutyronitrile, was obtained from Fluka A.G. (Buchs, Switzerland) and used as an initiator after recrystallization from methanol. The other chemicals were of ananalytical grade and were bought from Merck AG (Darmstadt, Germany). Distilled water was used in adsorption and desorption experiments. The sample and buffer solutions were pre-filtered with a 0.2 μm membrane (Sartorius, Göttingen, Germany).

2.2. Synthesis of [poly(EGDMA-VIM)] microspheres

VIM and EGDMA were polymerized in suspension with PVAL (used as the stabilizer) and AIBN (used as the initiator). Toluene (as a pore former) was used in the polymerization process as the diluent [31]. The polymerization conditions for the polymer microspheres are listed in Table 1. The continuous phase and dispersion phases were prepared by dissolving 200 mg of PVAL into 50 ml of purified water and by stirring 4 ml of toluene and 6 ml of EGDMA (30 mmol) together for 15 min at room temperature, respectively. After 100 mg of AIBN and 3 ml of VIM (30 mmol) were dissolved in the organic phase and homogenized, the prepared organic phase was stirred at 400 rpm for dispersion in the aqueous phase. The mixture was heated to 70°C for 4 h and then stirred at 600 rpm and 90°C for 2 h for the polymerization process [32]. To remove monomers or diluents retained in the polymer matrix,the prepared *[poly(EGDMA-VIM)]* microspheres were extensively washed with solvents such as, water and ethanol, and then dried in a vacuum oven at 50°C. The schematic illustration for suspension polymerization of the polymer microspheres is given in Fig. 1.

2.3. Characterization of the polymer microspheres

X-ray diffraction (XRD) patterns of the *[poly(EGDMA-VIM)]* microspheres were obtained with a X-ray diffractometer (Rigaku Ultima IV). The experimental conditions were scanned at 1°/min, and copper K alpha (CuKα) radiation was generated at a voltage of 40 kV and a current of 30 mA. Fourier transformation infrared (FTIR) spectra of the polymer microspheres were recorded with a Bruker Tensor 27 spectrophotometer. The spectra were obtained with Diamond-Attenuated Total Reflectance (ATR) in the 4000–400 cm^{-1} range, over 30 scans with a resolution of 2 cm^{-1}. Thermogravimetric (TG) analysis of the

Table 1
Polymerization conditions for synthesis of the *[poly(EGDMA–VIM)]* microspheres

Polymerization conditions	Stirring rate,temperature and time:
	400 rpm, 70°C, 4 h
	600 rpm, 90°C,2 h
	Reactor volume: 100 mL
Aqueous dispersion phase	PVAL: 200 mg
	Toluene: 4 mL
	Purified water: 50 mL
	EGDMA: 6.0 mL
Organic phase	AIBN: 100 mg
	VIM: 3 mL

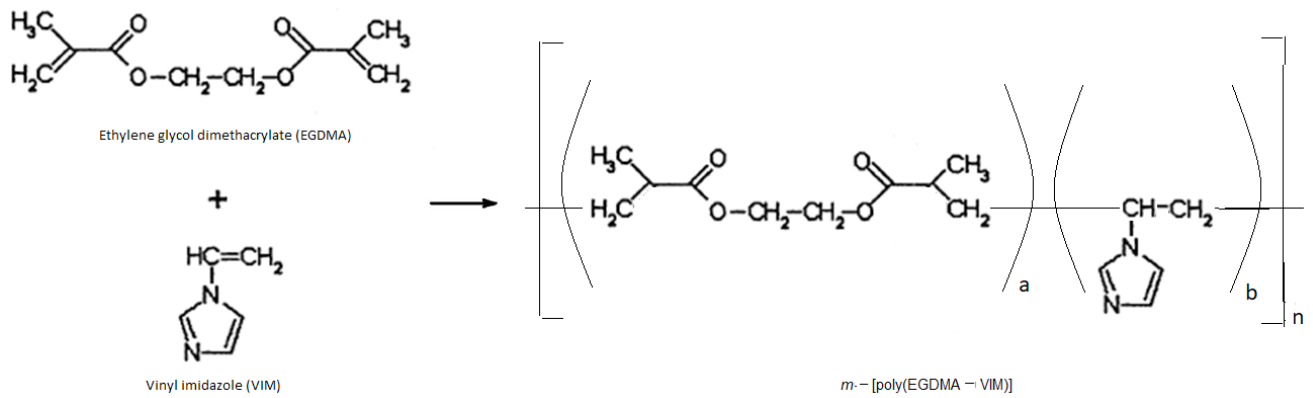

Fig. 1. Polymerization scheme for the preparation of the *[poly(EGDMA–VIM)]* microspheres [32].

polymer microspheres was conducted with a SETARAM-Labsys Thermogravimetric and Differential Thermal Analysis (TG-DTA) system at 10°C min^{-1} between 25°C and 950°C under air atmosphere. The surface morphology of the samples sputter-coated with gold was investigated with a QUANTA 400F Field Emission Scanning Electron Microscope (FESEM) system equipped with an energy dispersive X-ray (EDX) spectrometer, including operations at an accelerating voltage of 20 kV. The internal structure of the prepared polymer microspheres was investigated using FEI Tecnai G2 Spirit Biotwin model high contrast transmission electron microscopy (CTEM) with a Lantan-Hexaboron Electron Gun at 120 kV. Pore volume and surface area of the polymer microspheres were measured by a Quantachrome Corporation, Autosorb-6 Analyzer with N_2 adsorption/desorption isotherms at 77 K. The sample was degassed at 100°C for 4 h before the measurements were taken. The BET specific surface area, micropore volume, pore size distribution, total pore volume, and mesopore volume of the *[poly(EGDMA-VIM)]* microspheres were measured with the software of the instrument. The C, N, and H contents of the synthesized polymer microspheres were specified with an elemental analyzer (LECO, CHNS-932). The zeta potential of the polymer microspheres was defined with a MALVERN Nano ZS90 by dispersing the microspheres in water at various pH levels. The particle-size distribution of the polymer microspheres was determined with a MALVERN Mastersizer 2000 by dispersing them in water. Absorption, dispersant refraction index, and particle refraction index were set at 0.1, 1.33, and 1.52, respectively. The X-ray photoelectron spectroscopy (XPS) analyses were performed with the PHI 5000 VersaProbe for chemical identification of the constituent elements. Sample surfaces were excited by X-ray radiation from a monochromatic Al source. All analyses except FTIR analysis were conducted in the METU Central Laboratory, Ankara.

2.4. Swelling behavior of the [poly(EGDMA-VIM)] microspheres

The dried polymer microspheres were carefully weighed (± 0.0001 g) and placed into a vial with 50 ml of distilled water. The vial was then placed into a thermostatic water bath at 25±0.5°C for 2 h. The wet *[poly(EGDMA-VIM)]* microspheres were removed from the vial containing distilled water and weighed after they were wiped with filter paper. Swelling ratios of the *[poly(EGDMA-VIM)]* microspheres were calculated from Eq. (1) [42]:

$$Swelling\ ratio(\%) = \left[\left(W_s - W_o / W_o\right)\right] \cdot 100 \quad (1)$$

where W_o and W_s are weights of the *[poly(EGDMA-VIM)]* microspheres before and after swelling in the water, respectively.

2.5. Adsorption experiments

The maximum wavelength of phenol solution (35 mg L^{-1}) is 269 nm, and the other measurements were carried out at the maximum wavelength of 269 nm. For a calibration plot, the absorbance of phenol solutions (10–55 mg l^{-1}) was measured, and the plot of absorbance versus concentration was linear for the studied concentration range. The correlation coefficient was found to be 0.9991. The adsorption kinetic experiments were performed to investigate the effects of temperature, solution pH, adsorbent dosage, and initial phenol concentrations on the adsorption process. According to the preliminary experiment, the contact time was approximately 60 min for the adsorption equilibrium. The effects of the solution pH, the adsorbent dosage, and the initial solution concentrations on phenol removal were studied in the ranges of 3–11, 20–50 mg, and 30–70 mg L^{-1}, respectively. pH of the phenol solutions were adjusted using 0.1 mol L^{-1} NaOH or HCl with a NeoMet pH-200 l pH meter. Phenol adsorption experiments were carried out at the range of 25–55°C in a constant temperature bath to specify the effects of temperature. The sample volumes were drawn from the suspension system at specified time intervals and filtered using syringe filters with 0.22 µm pores. After the adsorption equilibrium was reached, residual phenol concentration in the solutions was determined by a UV-Vis spectrophotometer (Shimadzu UV-2450) at 269 nm. The amount of phenol adsorbed at contact time was obtained from Eq. (2) [32]:

$$q_{t=} \frac{\left(C_o - C_t\right) \cdot V}{m} \quad (2)$$

In Eq. (1), m (g), V (L), q_t (mg g^{-1}), C_0, and C_t (mg L^{-1}) are the weight of the dried *[poly(EGDMA-VIM)]* microspheres and phenol solution volume, the adsorption capacity of the polymer microspheres, and the initial and equilibrium concentrations of phenol.

2.6. Regeneration of the [poly(EGDMA-VIM)] microspheres

When the novel adsorbent is synthesized, simple regeneration process and adsorbate isolation are very important due to decreasing costs and the repeated use of the adsorbent [43]. Reusability of the adsorbents after the regeneration process is the most effective parameter to decide whether to use the adsorbents in the waste-water treatment systems and on an industrial scale [4,40,41]. It was reported in the literature that the best elution of phenol from various adsorbents was obtained using NaOH solutions [4,28,43]. Therefore, after the adsorption of phenol, 50 mL of 0.01 M NaOH solution was used for the regeneration of the *[poly(EGDMA-VIM)]* microspheres. The polymer microspheres were washed with distilled water after the desorption process and then reused in the sequential phenol adsorption-desorption cycles 5 times. The process of phenol adsorption and desorption were performed at 25°C at a pH of 5.47 and 50 mg of adsorbent dosage. The desorption efficiency (%) was determined using Eq. (3) [23]:

$$\text{Desorption efficiency}(\%) = \frac{\text{amount of phenol desorbed}}{\text{amount of phenol adsorbed}} \cdot 100 \qquad (3)$$

3. Results and discussion

3.1. Characterization of the [poly(EGDMA-VIM)] microspheres

Elemental analysis was performed to determine the composition of the prepared polymer microspheres and the obtained data are given in Table 2. The results of elemental analysis showed that *N* content of the polymer microspheres is 0.8%. In polymerization, *VIM* and *AIBN* contain *N*, and the percentage of total *N* content used for suspension polymerization is 1.52% (1.47% from VIM and 0.05% from *AIBN*). According to the *N* content of the polymer microspheres, the main *N* content was formed by *VIM*, and some *VIM* monomers did not attend to the structure of the polymer microspheres due to removal by extensive washing. In addition, the amount of *VIM* in the *[poly(EGDMA-VIM)]* microspheres was determined as 83.42 mmol g^{-1} from the stoichiometry of nitrogen by using the data in Table 2. The elemental analysis provides direct evidence of formation of the polymer microspheres.

The *[poly(EGDMA-VIM)]* microspheres are insoluble in water due to their crosslinked structure [32]. However, they exhibit swelling properties that are affected by the cross-linking degree of the polymer microspheres and the hydrophilicity of the polymer matrix [40,41]. The swelling test showed that the equilibrium swelling ratio of the synthesized polymer microspheres is 53%. A previous study revealed that the swelling ratios decrease with increased *VIM* and cross-linker content because of the decrease in hydrophilicity of the structure [40]. According to the explanation, hydrophobicity of the *[poly(EGDMA-VIM)]* microspheres is high; therefore, the water molecules in aqueous solutions cannot penetrate the tortuosity polymer chains easily.

Table 2
Elemental analysis data of the *[poly(EGDMA–VIM)]* microspheres

	[poly(EGDMA–VIM)] microspheres
C%	58.74
H%	7.41
N%	0.80

The adsorption-desorption isotherm and pore-size distribution of the polymer microspheres is given in Fig. 2a. The specific surface area and porous structure of the polymer microspheres were studied by measuring N_2 adsorption-desorption isotherms at 77 K. The BET surface area for the *[poly(EGDMA-VIM)]* microspheres is 304.4 $m^2 g^{-1}$. Their surface area is 5 times higher than that of the polymer beads synthesized in the previous studies [31–34]. The adsorption-desorption isotherm of the polymer microspheres can be classified as a type-IV isotherm according to IUPAC classification [1], and they exhibited an H_3-type hysteresis loop in the mesopore range. From the adsorption-desorption isotherm, it can be seen that N_2 molecules first diffuse into the micropore under extremely low pressure, and the adsorption capacity then increases with the increase in relative pressure due to the monolayer/multilayer adsorptions of N_2 molecules on the mesopores [42]. The pore-size distribution (inset in Fig. 2a) calculated from the Barret-Joyner-Halende (BJH) model and change in pore sizes of the polymer microspheres in the range of 1.9 nm (micro) to 7.8 nm (meso) show that the *[poly(EGDMA-VIM)]* microspheres contain micropores and mesopores.

Phase investigation of the *[poly(EGDMA-VIM)]* microspheres was performed by XRD, and the XRD pattern of the polymer microspheres is given in Fig. 2b. As the pattern shows, the polymer microspheres have a mean peak at 2θ angles between 10° and 25°, and the broad reflection peak is attributed to the amorphous polymer microspheres.

The structural characterization of the polymer microspheres was performed by FTIR spectroscopy, and Fig. 2c shows their FTIR spectra. The presence of the peaks at 2,991 and 2,955 cm^{-1} are assigned to the C–H asymmetric stretching of $-CH_2-$ and $-CH_3-$ in the polymer chain, respectively. Segatelli et al. reported the similar peaks for the C–H asymmetric stretching at 2,988 and 2,960 cm^{-1} in 2010 [36]. The peaks at 1,151 and 1,251 cm^{-1} and the peak with high intensity at 1,726 cm^{-1} can be referred to the C–O stretching and the C=O vibration of the ester group of *EGDMA*, respectively. The C=O vibration of the ester group of *EGDMA* was noted at 1,720, 1,738 and 1,721 cm^{-1} by Kara et al. in 2004 [32], Segatelli et al. in 2010 [36], and Tarley et al. in 2015 [37], respectively. The characteristic peaks of imidazole ring in the polymer microspheres appear at 1643 cm^{-1} (stretching of C=C and C=N), 1,458cm^{-1} (stretching of C–C and C–N), 1,390 cm^{-1} (the C–N stretching modes for the ring), and 954 cm^{-1} (in-plane ring C–H bending) [32]. In 2015, Tarley et al. reported the similar FTIR peaks of imidazole ring at 1,638, 1,487 and 1,386 cm^{-1} [37]. Therefore, the results of the FTIR analysis verified that the *[poly(EGDMA-VIM)]* microspheres were

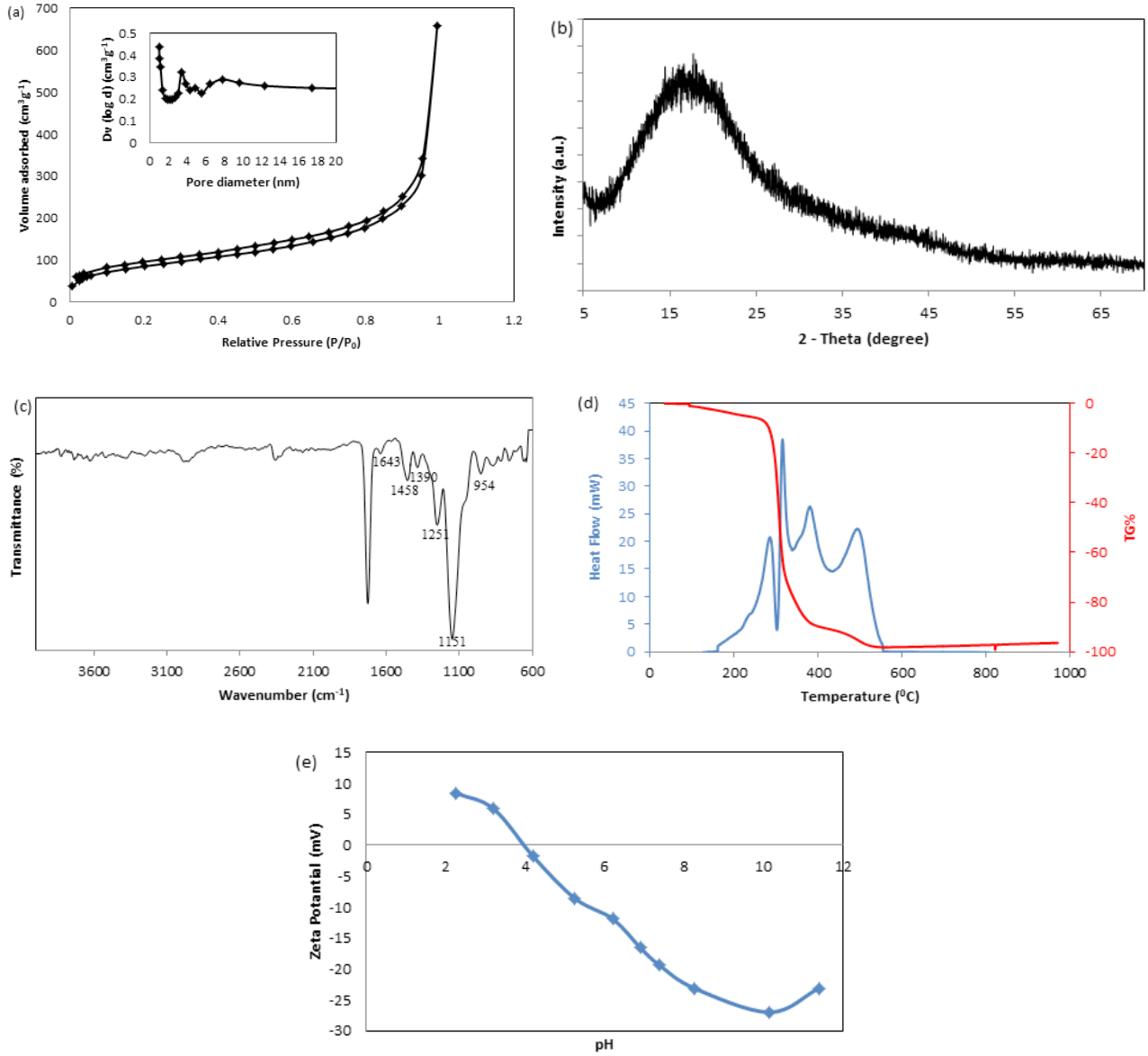

Fig. 2. (a) N_2 adsorption-desorption isotherm and pore-size distribution (inset) (b) XRD pattern (c) FTIR spectra (d) TGA and DTA curves (e) Zeta potential of the *[poly(EGDMA–VIM)]* microspheres.

prepared with the participation of *VIM* in the structure of the polymer microspheres.

Fig. 2d shows the thermal degradation behaviors of the *[poly(EGDMA-VIM)]* microspheres. A mass loss of 4.15% can also be detected at up to 200°C because of the loss of adsorbed water molecules. Weight loss occurred stepwise in the ranges of 200–300°C, 300–350°C, 350–415°C, and 415–550°C in the *[poly(EGDMA-VIM)]* microspheres. The first and second steps with maximum degradation temperatures of 285.58 and 315.29°C, respectively are due to the thermal degradation of poly(ethylene glycol dimethacrylate) segments [36,37]. The DTA curve for the polymer microspheres reveals the surprising occurrence of an endothermic effect at 301.93°C and the sharp endothermic peak is due to thermal degradation of *[poly(EGDMA-VIM)]* which is a cross-linked polymer matrix [44]. The third and fourth steps with maximum degradation temperatures of 381.03 and 493.33°C, respectively, are referred to the decomposition of poly(vinylimidazole). Similar results for degradation temperatures of poly(ethylene glycol dimethacrylate) (200–300°C) and poly(vinylimidazole) (300–450°C) segments were observed by Segatelli et al. [36] and Tarley et al. [37]. As Fig. 2d shows, the percentage of weight loss for the *[poly(EGDMA-VIM)]* microspheres appearing at the first, second, third, and fourth decomposition steps were determined to be 22.93, 54.11, 9.24, and 7.75 wt.%, respectively. At 550°C, the thermal decomposition of the synthesized polymer microspheres can be considered complete, and the total weight loss is 98.18%.

To investigate surface potential, zeta potential of the prepared polymer microspheres was measured as a function of the pH, and the curve is reported in Fig. 2e. The zeta potentials play an important role in the measurement of attractive

or repulsive forces between adsorbate and adsorbent. The isoelectric point of the *[poly(EGDMA-VIM)]* microspheres is 3.95. The surface of the *[poly(EGDMA-VIM)]* microspheres is positively charged in an acidic condition (pH < 4) and negatively charged in neutral and basic conditions (pH > 4).

The morphology of the polymer microspheres was determined by SEM and TEM analysis, and their SEM micrographs and TEM images are given in Figs. 3a–d, which shows the SEM micrographs and internal surface of a single polymer microsphere. The polymer microspheres have a fine spherical shape with a diameter of 40 μm. In Fig. 3b, the *[poly(EGDMA-VIM)]* microspheres show a lower degree of aggregation during the polymerization process and the variation in size of the polymer microspheres. In 2009 Uğuzdoğan et al. [40] reported that the microspheres have a nonporous structure because no pore is present at the surface or cross-sectional views of the PEGMA-VI microspheres. The *[poly(EGDMA-VIM)]* microspheres synthesized in this study have a rough surface (Figs. 3a and 3b), which may result in higher surface area. A similar porous structure was observed among the *[poly(EGDMA-VIM)]* microspheres in our previous studies [32,34]. The inequality on surface of the *[poly(EGDMA-VIM)]* microspheres is important for adsorption processes and promotes a higher contaminant adsorption [36].

In Fig. 3c, the distribution of the polymer microspheres is uniform without any secondary agglomeration, and the polymer microspheres' diameters vary. The *[poly(EGDMA-VIM)]* microspheres are well-defined and have a spherical shape and porous structure (see Fig. 3d). Additionally, the TEM image in Fig. 3d illustrates that the average diameter of single polymer microsphere is approximately 130 nm. The results of TEM analysis show that the polymer microspheres have been prepared by suspension polymerization.

The particle-size distribution of the *[poly(EGDMA-VIM)]* microspheres is shown in Fig. 3e. Their particle-size distribution was determined with the dynamic light scattering (DLS) technique. Fig. 3e shows only one distinct peak at around 69 μm for the polymer microspheres, very broad particle-size distribution, and a monomodal distribution with no aggregation in the sample. Kara et al. in 2004 [32] and Uğuzdoğan et al. in 2009 [40] reported the particle size range as 150 to 200 μm for the *[poly(EGDMA-VIM)]* microspheres and 10 to 50 μm for the PEGMA-VI microspheres, respectively. Additionally, Uğuzdoğan et al. [40] reported that the final product's average size ranges from 50 to 1000 μm, but the *[poly(EGDMA-VIM)]* microspheres' sizes ranged from 0.48 to 275.42 μm in this study. This range was confirmed by the SEM micrograph and TEM image (Figs. 3a–d). The result can be explained by the polarity of *VIM* groups and lower surface tension of water-insoluble diluent [40].

3.2. Adsorption of phenol onto the [poly(EGDMA–VIM)] microspheres

3.2.1. Effects of adsorbent dosage; contact time; and initial phenol concentration, pH, and temperature

The effects of adsorbent dosage; contact time; and initial phenol concentration, pH, and temperature on the phenol removal with the *[poly(EGDMA-VIM)]* microspheres is given in Figs. 4a–d. To investigate the adsorbent dosage effect, phenol adsorption experiments using various amounts of adsorbent (20, 30, 40, and 50 mg) were performed. Fig. 4a shows that phenol adsorption increased along with adsorbent dosage, from 20 to 50 mg, and the volume and concentration of the solution remained constant. The result was an increase in the number of active adsorption sites on the *[poly(EGDMA-VIM)]* microspheres' surface [45]. Similar behavior was observed in a previous biosorption study of phenol from aqueous solutions onto chitosan-calcium alginate blended beads [25]. Therefore, 50 mg of adsorbent was used in the following adsorption experiments.

Fig. 4b shows that phenol adsorption onto the polymer microspheres is very fast for 20 min and then slows near the equilibrium. The equilibrium time is almost 90 min. This result may be explained by the abundant number of active sites on surface of the *[poly(EGDMA-VIM)]* microspheres available for phenol adsorption at the initial stage, but then it becomes difficult because of the active sites' saturation on surface of the polymer microspheres [2]. In this study, it was found that the removal rate of phenol by the *[poly(EGDMA-VIM)]* microspheres is faster than that by various adsorbents that were reported in the literature [1,21,25]. The increase in the initial concentration of phenol solution results in a longer time to reach adsorption equilibrium because of the competition of phenol molecules in aqueous solution and repulsive forces between the phenol molecules on the polymer microspheres and bulk phases [45,46]. It was also found that increasing the initial concentration of phenol solution resulted in increased phenol removal (Fig. 4b). This result could occur because the phenol concentration in the solution increases the mass transfer driving force and, hence, the rate at which phenol molecules pass from the bulk solution to the *[poly(EGDMA-VIM)]* microspheres [14]. Similar trends were reported for phenol removal onto various adsorbents [1,4,14,45].

The effect of initial pH on phenol adsorption with the polymer microspheres was measured in the adsorption experiments in the initial pH range of 5.47–11 of the solutions. Phenol adsorption onto the *[poly(EGDMA-VIM)]* microspheres is strongly affected by initial pH due to ionization of adsorbate and surface charge of adsorbent. Fig 4c shows that the adsorption capacity of phenol onto the polymer microspheres decreased as the initial solution pH increased. The anionic state of phenol increases as pH increases [4,21]. Moreover, the isoelectric point of the *[poly(EGDMA-VIM)]* microspheres is 3.95 (in Fig. 2e). Therefore, surfaces of the polymer microspheres are negatively charged in neutral and basic circumstances (pH value > isoelectric point). The phenol adsorption is reduced because of repulsion between the polymer microspheres with negatively charged surfaces and the anionic phenol. Phenol is a weak acid (pKa = 10) [14], and the entity of ionic and molecular forms of phenol in an aqueous solution depends on the solution's pH value [47]. The adsorption capacity of the polymer microspheres was low at a pH of 3 and coincided with a pH of 7 due to the protonation of nitrogen atoms at the vinylimidazole (pKa = 6.26) [37] in the microspheres' structures and lower solubility of phenol in acidic conditions [4]. Therefore, the hydrogen bond between the surfaces of the polymer microspheres and phenol hydroxyl groups becomes less possible. The adsorption

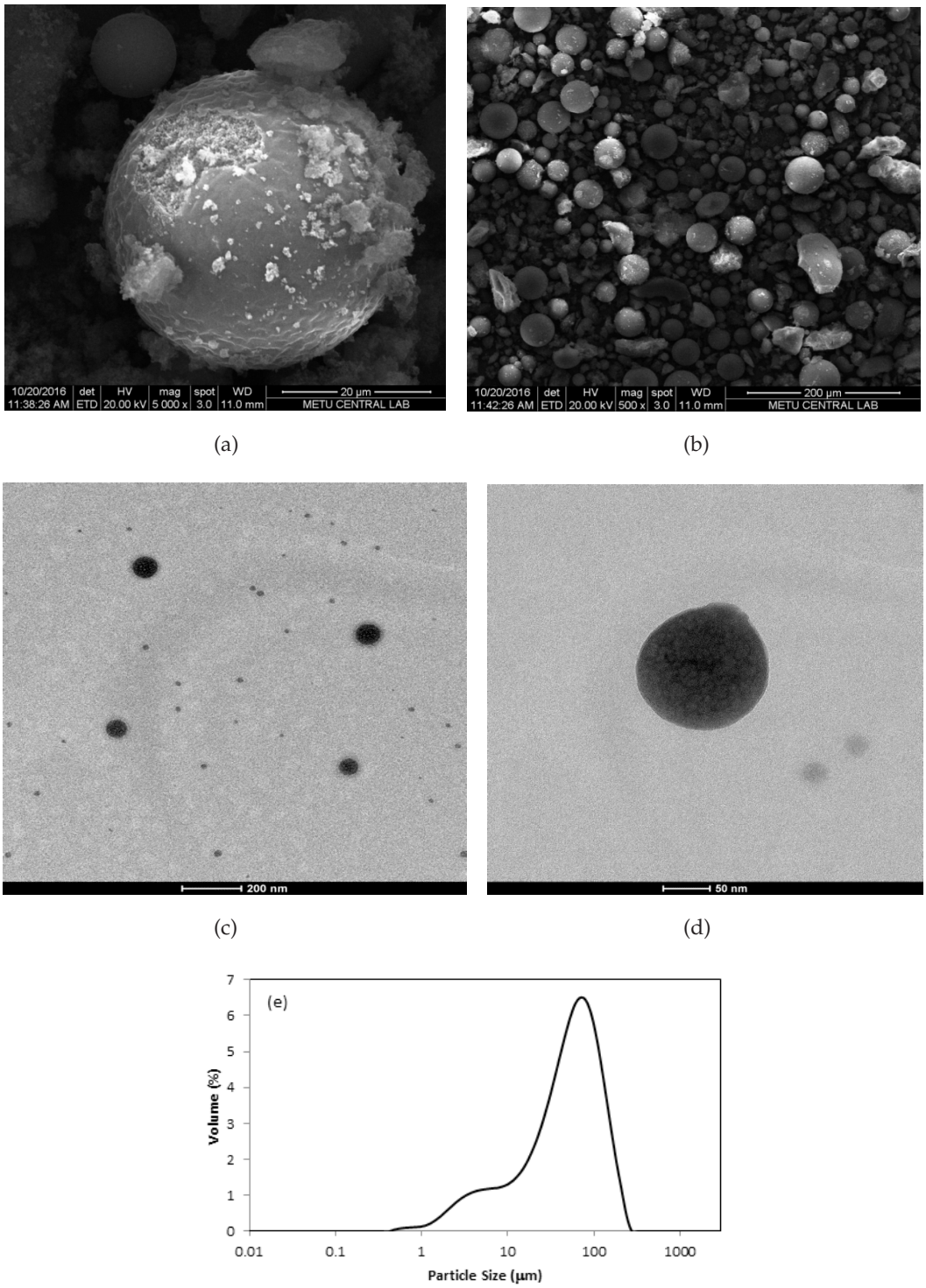

Fig. 3. SEM micrographs (a) 20 µm (b) 200 µm, TEM images (c) 200 nm (d) 50 nm, (e) the particle size distribution for the *[poly(EGDMA–VIM)]* microspheres.

capacity of the polymer microspheres provides a maximum value at a pH of 5.47 because of the molecular form of phenol in the solutions and the deprotonation of nitrogen atoms in the vinylimidazole in the polymer microspheres structure around a pH of 6 [37]. Therefore, potent hydrogen bonds exist between the surfaces of the *[poly(EGDMA-VIM)]* microspheres and phenol hydroxyl groups,which are favorable for adsorption at pH < pKa. The same behavior was observed and reported for various adsorbents in related literature [4,14,25]. Therefore, further experiments for phenol adsorption were conducted at an initial a pH of 5.47, which is the natural pH of phenol solution.

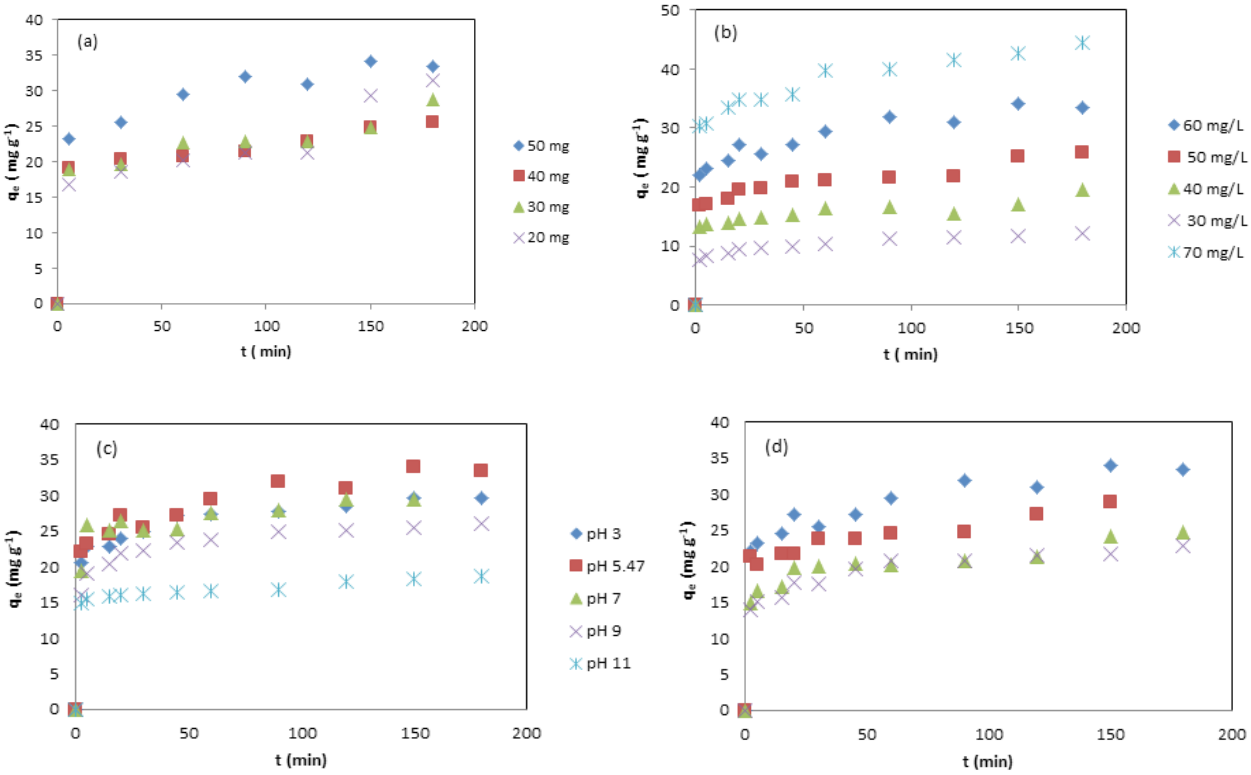

Fig. 4. Effects of (a) adsorbent dosage (natural pH, pH = 5.47, temperature of 25°C, phenol concentration of 60mg L^{-1}) (b) contact time and initial concentration (natural pH, temperature of 25°C, adsorbent dosage of 50 mg g^{-1}) (c) pH (Adsorbent dosage of 50 mg g^{-1}, temperature of 25°C, phenol concentration of 60 mg L^{-1}) (d) temperature (Natural pH, phenol concentration of 60 mg L^{-1}, adsorbent dosage of 50 mg g^{-1}) (◆25°C ■35°C ▲45°C ×55°C) on phenol removal using the *[poly(EGDMA-VIM)]* microspheres.

To investigate the effect of temperature on phenol adsorption onto the *[poly(EGDMA-VIM)]* microspheres, phenol adsorption experiments were performed at 25, 35, 45 and 55°C. The results are shown in Fig. 4d. The amount of phenol adsorbed decreased from 33.39 to 22.77 mg g^{-1} as the temperature increased from 25 to 55°C. Similar trends were reported for phenol removal onto a few adsorbents, such as thermal modified activated carbon [48] and acrylic ester-based crosslinked resin [49], whereas the opposite trends were observed for most of the adsorbents [43,45,50]. This result could have occurred because the adsorptive forces between phenol molecules and the active sites on the surface of the *[poly(EGDMA-VIM)]* microspheres decrease as the temperature increases [48,49]. Additionally, it was found that the adsorption process is exothermic due to the decrease removal of phenol with an increase in temperature. In Fig. 4d, the diffusion rate of the phenol molecules in the solution and hence the adsorption equilibrium time was expedited with the increase in temperature [45].

3.2.2. Adsorption kinetics

The pseudo-first-order, pseudo-second-order and intra-particle diffusion models were implemented with adsorption experimental data which were determined from Fig. 4d at various temperatures to interpret the kinetic parameters for these models. The equations of kinetic models were expressed in Eqs. (4), (5), and (6) [1,4,45];

$$\ln\left(q_e - q_t\right) = \ln q_e - k_1 t \tag{4}$$

$$\frac{t}{q_t} = \frac{1}{k_2 q_e^2} + \frac{t}{q_e} \tag{5}$$

$$q_t = k_{id} x t^{1/2} + C \tag{6}$$

where q_t (mg g^{-1}) and q_e (mg g^{-1}) are the amount of phenol adsorbed onto the *[poly(EGDMA-VIM)]* microspheres at time t (min) and equilibrium, respectively; C (mg g^{-1}) is a constant; and k_1 (min^{-1}), k_2 (g mg^{-1} min^{-1}), and k_{id} (mg g^{-1} $min^{-1/2}$) are the pseudo-first-order, pseudo-second-order, and intra-particle diffusion rate constants, respectively. The plot of t/q_t versus t obtained for phenol adsorption onto the polymer microspheres at various temperatures is illustrated in Fig. 5. The values of k_1 and q_e, k_2 and q_e, and k_{id} and C were calculated with the slopes and intercepts of the plots of $ln\ (q_e - q_t)$ versus t, t/q_t versus t, and q_t versus $t^{1/2}$, respectively. The determined kinetic parameters are given in Table 3.

As Table 3 shows, the calculated q_e values by intra-particle diffusion and pseudo-first-order kinetic equations were lower than the experimental q_e values, and the correlation coefficients for these kinetics models were relatively low. These results indicate that the adsorption of phenol onto the polymer microspheres is not suitable for the intra-particle diffusion and pseudo-first-order kinetic. In Table 3,

the q_e values calculated at various temperatures by the pseudo-second-order kinetic model were consisted with the experimental q_e values, and the correlation coefficients determined for four temperatures were extremely high. The pseudo-second-order model is more likely to predict that in the kinetic behavior of adsorption, the rate-limiting step may be controlled by valence forces by the sharing or exchanging of electrons between adsorbent and adsorbate [25,43,48]. As a result, phenol adsorption onto the *[poly(EGDMA-VIM)]* microspheres is suitable for the pseudo-second-order kinetic, and phenol adsorption is probably due to the interaction between the π electrons in phenolic ring of phenol and the basal plane of the polymer microspheres [48]. This conclusion is also supported with discussion of the adsorption mechanism. According to previous studies, the adsorption kinetics of phenol onto various adsorbents was also fitted by the pseudo-second-order kinetic model [4,21,43,45]. The intra-particle diffusion model was studied in order to determination of the rate-limiting step (external surface adsorption, intra-particle diffusion, or adsorption at the active site) [50]. When the plot of q_t versus $t^{1/2}$ passed through the origin, the rate-limiting step was the intra-particle diffusion of the adsorbate molecules into the pores of adsorbent [4]. The plots of q_t versus $t^{1/2}$ [from Eq. (6)] do not pass through the origin or the *C* values, which show the thickness of the diffusion boundary layer is not the zero point at various temperatures; therefore, besides the intra-particle diffusion model, some other mass transfer mechanisms occur during the removal of phenol by the *[poly(EGDMA-VIM)]* microspheres. A similar observation was reported by Nadavala et al. [25], Gao et al. [45], and Cheng et al. [50] for phenol removal.

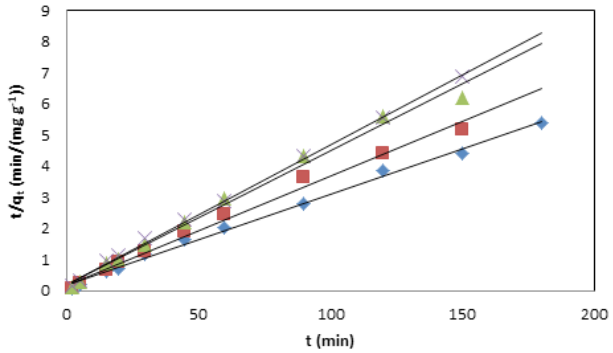

Fig. 5. The fitting of pseudo-second-order model for the adsorption of phenol onto the *[poly(EGDMA–VIM)]* microspheres (phenol concentration of 60 mg L^{-1}, natural pH, adsorbent dosage of 50 mg g^{-1}) (◆25°C ■35°C ▲45°C ×55°C).

Table 3 shows that the k_2 values increase as the solution temperature increases. The linear relationship between temperature and the k_2 was determined with the following Arrhenius-type relationship [51]:

$$\ln k_2 = \ln k_0 - \frac{E_a}{RT} \tag{7}$$

In Eq (7), k_2 (g mg^{-1} min^{-1}) and k_0 (g mg^{-1} min^{-1}) are the pseudo-second-order rate constants and the independent temperature factor, respectively. T is the solution temperature (K), E_a is the activation energy for phenol adsorption (kJ mol^{-1}), and R is the gas constant (8.314 J mol^{-1} K^{-1}). In Eq. (7), E_a and k_0 are calculated as 21.003 kJ mol^{-1} and 22.800 g mg^{-1} min^{-1} by a linear method. For the adsorption process, E_a was less than 25–30 kJ mol^{-1} for the diffusion-controlled process [51]. Therefore, the rate of phenol adsorption onto the *[poly(EGDMA-VIM)]* microspheres is controlled by the diffusion process.

3.2.3. Adsorption isotherms

The Freundlich, Langmuir and Dubinin-Radushkevich isotherms models were investigated to define the equilibrium characteristics of phenol adsorption onto the prepared polymer microspheres. The linear forms of these isotherm equations can be represented in Eqs. (8), (9), and (10) [23];

$$\ln q_e = \ln K_F + \frac{1}{n}\ln C_e \tag{8}$$

$$\frac{C_e}{q_e} = \frac{1}{K_L q_m} + \frac{C_e}{q_m} \tag{9}$$

$$\ln q_e = \ln q_m - K_{D-R}\left[RTln\left(1+\frac{1}{C_e}\right)\right]^2 \tag{10}$$

where q_e (mg g^{-1}) is the amount of phenol adsorbed onto the *[poly(EGDMA-VIM)]* microspheres at equilibrium, q_m (mg g^{-1}) is the maximum adsorption capacity, C_e is the equilibrium concentration (mg L^{-1}) of phenol, K_F ($mg^{1-1/n}$ $L^{1/n}$ g^{-1}) and n are the Freundlich adsorption coefficient and exponent, respectively; K_L (L mg^{-1}) is the Langmuir constant; and K_{D-R} (mol^2 J^{-2}) is the Dubinin-Radushkevich constant. The calculated isotherm parameters and the correlation coefficients are shown in Table 4.

Table 3
Kinetic parameters for phenol adsorption onto the *[poly(EGDMA–VIM)]* microspheres

T (K)	$q_{e,experimental}$ (mg g^{-1})	Pseudo-first-order			Pseudo-second-order			Intra-particle diffusion		
		k_1 (min^{-1})	q_e (mg g^{-1})	R^2	k_2 (g mg^{-1} min^{-1})	q_e (mg g^{-1})	R^2	k_{id} (mg g^{-1} $min^{-1/2}$)	C (mg g^{-1})	R^2
298	33.3962	0.0157	10.6963	0.8332	0.0046	34.2466	0.9954	0.9884	21.1360	0.9414
308	28.8679	0.0113	8.4587	0.9010	0.0063	28.4900	0.9919	0.7101	19.1790	0.9218
318	24.7169	0.0078	7.4633	0.7263	0.0088	23.3100	0.9908	0.6790	15.1540	0.8601
328	22.7673	0.0170	9.1641	0.8459	0.0097	22.2717	0.9984	0.7477	13.6460	0.9209

Table 4
Isotherm constants for phenol adsorption onto the *[poly(EGDMA–VIM)]* microspheres

Isotherm	Constants	Temperature			
		25°C	35°C	45°C	55°C
Langmuir	$q_{m,exp.}$ (mg g^{-1})	33.3962	28.8679	24.7169	22.7673
	q_m (mg g^{-1})	34.7441	30.2093	26.9388	24.2211
	K_L (L mg^{-1})	0.0618	0.0496	0.0387	0.0348
	R^2	0.9860	0.9879	0.9720	0.9845
Freundlich	n	0.9139	0.7114	0.5102	0.4403
	K_F ($mg^{1-1/n}$ $L^{1/n}$ g^{-1})	1.1864	3.5045	25.3365	84.8805
	R^2	0.9877	0.9912	0.9837	0.9921
Dubinin-Radushkevich	q_m (mg g^{-1})	32.9733	24.4001	24.4439	28.3099
	K_{D-R} (mol^2 J^{-2})	$8x10^{-9}$	$1x10^{-8}$	$2x10^{-8}$	$3x10^{-8}$
	E (kJ mol^{-1})	2.5000	2.2361	1.5811	1.2909
	R^2	0.9559	0.9714	0.9556	0.9800

Table 4 shows that the Freundlich isotherm had a better fit with the phenol adsorption data than Langmuir and Dubinin-Radushkevich isotherms due to their higher correlation coefficient (R^2) value. The Freundlich isotherm is based on the assumption that the adsorption occurs on heterogeneous sites with nonuniform distribution of energy levels. The Freundlich isotherm describes reversible adsorption and is not restricted to the formation of a monolayer [4]. A value of 1/n > 1 suggests a weak adsorption bond between phenol molecules on the polymer microspheres, and the surfaces of the *[poly(EGDMA-VIM)]* microspheres are heterogeneous due to a Freundlich constant, *n*, less than 1 [49,50]. According to previous studies, the adsorption isotherms of phenol onto various adsorbents can also be fitted with the Freundlich isotherm model [4,49,50]. One could deduce that phenol adsorption onto the *[poly(EGDMA-VIM)]* microspheres fits the characteristics of heterogeneous surface adsorption.

The equilibrium data of phenol adsorption were fitted into the Dubinin-Radushkevich isotherm model to determine the type of phenol adsorption (chemical or physical adsorption) onto the *[poly(EGDMA-VIM)]* microspheres. The *E* (mean sorption energy) values, which give information about the mechanism of the adsorption process as physical adsorption or chemical ion-exchange, can be calculated from K_{D-R} [25];

$$E = \frac{1}{\sqrt{2K_{D-R}}} \tag{11}$$

The mean free energy of adsorption values, *E*, calculated from Eq. (11) for various temperatures are listed in Table 4. If the adsorption process follows a chemical ion exchange, the value of *E* is between 8 and 16 kJ mol^{-1} whereas if the value of *E* is <8 kJ mol^{-1}, the adsorption process is physical adsorption [25]. For phenol removal onto the *[poly(EGDMA-VIM)]* microspheres, the mean adsorption energy (*E*) values were calculated as 2.5000, 2.2361, 1.5811 and 1.2909 at 25, 35, 45, and 55°C, respectively. These values indicate that the process of phenol adsorption can be estimated as physical adsorption ($E < 8$ kJ mol^{-1}) at various temperatures.

3.2.4. Adsorption thermodynamics

The thermodynamics of phenol adsorption were obtained following Van't Hoff equations [50,52,53];

$$\Delta G^\circ = -RTlnK_D \tag{12}$$

$$\lim_{C_e \to 0} \frac{q_e}{C_e} = K_D \tag{13}$$

$$\Delta G^\circ = \Delta H^\circ - T\Delta S^\circ \tag{14}$$

In Eqs. (12), (13), and (14), K_D is the adsorption equilibrium constant, and *T* and R are the temperature and universal gas constant (8.314 J mol^{-1} K^{-1}), respectively. K_D can be determined from the intercept of the plot of $ln\ (q_e/C_e)$ vs. C_e (not shown) [52]. ΔH°, Δ*S*°, and Δ*G*° are the enthalpy change, the entropy change and the free energy change of the phenol adsorption, respectively.

Eq. (15) can be determined using Eqs. (12) and (14) [50,52,53];

$$\ln K_D = \frac{\Delta S^\circ}{R} - \frac{\Delta H^\circ}{RT} \tag{15}$$

The slope and intercept of the plot of $ln\ K_D$ versus *1/T* (not shown) were used to determine the values of Δ*H*° and Δ*S*°, respectively.

The thermodynamic parameters calculated for the phenol adsorption are listed in Table 5. The values of ΔG° are −2.231, −2.116, −2.001, and −1.886 kJ mol^{-1} at 298, 308, 318, and 328 K. respectively. The results showed that the phenol adsorption onto the *[poly(EGDMA-VIM)]* microspheres is favorable at lower temperatures and occur spontaneously [52,53]. For physisorption, Δ*G*° is usually between −20 and 0 kJ mol^{-1}, and Δ*H*° is less than 40 kJ mol^{-1} [53,54]. The values of ΔG° indicated that the phenol adsorption onto the polymer microspheres is physisorption. The value of Δ*H*° is−5.659 kJ mol^{-1}, and phenol adsorption is an exothermic process. The negative Δ*H*° value is less than 40 kJ mol^{-1}.Therefore, phenol adsorption onto the prepared polymer microspheres is

Table 5
The thermodynamic values of the phenol adsorption onto the *[poly(EGDMA–VIM)]* microspheres at different temperatures

Solution temperature (K)	ΔG° (kJ mol^{-1})	ΔH° (kJ mol^{-1})	ΔS° (J mol^{-1} K^{-1})
298	–2.231	–5.659	–11.504
308	–2.116		
318	–2.001		
328	–1.886		

a physical process [48]. The negative value of ΔS° shows the freedom degree at the solid/solution interface decreases during phenol removal [52,53]. Similar results for phenol adsorption thermodynamics were reported by Zhang et al. [48] and Qiu et al. [49].

3.2.5. Regeneration and reusability of the [poly(EGDMA-VIM)] microspheres

Simple regeneration is a very important goal for the development of new adsorbents due to the adsorbents' decreasing costs and repeated use [4,28,43]. Additionally, the feasibility of adsorption process depends greatly on the cost of regeneration of used adsorbents. Regeneration can be performed by thermal regeneration or solvent regeneration [14]. In this study, the desorption of phenol from the loaded *[poly(EGDMA-VIM)]* microspheres with a 0.01 M NaOH solution was an effective treatment. The desorption efficiency was found to be greater than 96% for 3 h because of the high solubility of the sodium salt of phenol in the aqueous solutions [43]. The adsorption/desorption cycle was conducted five times to interpret and demonstrate the reusability of the *[poly(EGDMA-VIM)]* microspheres. The results are shown in Fig. 6, which shows that the adsorption capacities of the polymer microspheres decreased from 33.15 to 29.69 mg g^{-1} after five cycles.

3.2.6. The performance of the [poly(EGDMA-VIM)] microspheres as adsorbent

The adsorption performance of the prepared polymer microspheres was compared to the various adsorbents reported in the literature for the removal of phenol. Table 6 shows that the *[poly(EGDMA-VIM)]* microspheresused in the present study exhibited strong adsorption capacity and could be regarded as an alternative adsorbent for the removal of phenol from aqueous solutions.

3.2.7. Adsorption mechanism

Adsorption mechanisms are very important to explain adsorption characteristics and define the equilibrium relationship between the adsorbate and the adsorbent. The phenol adsorption onto the polymeric adsorbent occurs because of the π-π interaction between the polymer chain and phenol, intermolecular hydrogen bonding and the electrostatic interaction [48,53,58]. In this study, to explain the adsorption mechanism,phenol adsorbed the polymer

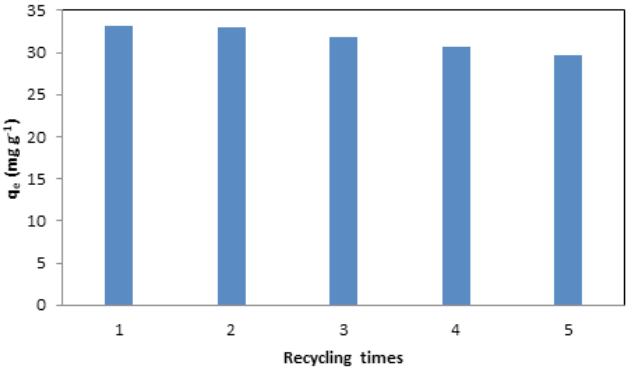

Fig. 6. Adsorption amounts of phenol on the *[poly(EGDMA–VIM)]* microspheres before and after regeneration at pH = 5.47.

Table 6
Comparison of the adsorption capacity determined from Langmuir isotherm of various adsorbents for phenol

Adsorbent	Max. adsorption capacities (mg g^{-1})	Refs.
Bentonite	1.17	[14]
SDS-alumina	6.60	[55]
Graphene oxide grafted with poly(N-isopropylacrylamide)	12.74	[56]
The carboxylic functionalized poly (glycidyl methacrylate)(PGMA)	20.80	[57]
The *[poly(EGDMA-VIM)]* microspheres	34.74	In this study
Zeolite X/activated carbon composite	37.92	[50]
Activated Semi coke	42.75	[45]
TBP/Fe_3O_4@PSF microcapsules	79.36	[4]
Chitosan-calcium alginate blended beads	108.69	[25]

microspheres were characterized with FTIR, XRD and XPS analysis.

Changes such as the decrease in band intensity or shifts in the FTIR peaks indicate interactions of functional groups on the *[poly(EGDMA-VIM)]* microspheres surface with phenol. Fig. 7a shows that after adsorbed phenol, a few new and weak absorption bands appear in the spectrum and the bands are typical for phenol and located at 1,561, 1,478, 1,076, and 813 cm^{-1} [59]. Apart from these bands, the spectrum presents a new peak at 762 cm^{-1} due to the benzene ring's vibration [60]. Additionally, the intensity and location of the peaks (C=C and C=N peaks) between 1,700 and 1,400 cm^{-1} changed after phenol adsorption due to the π-π interaction between the polymer chain and phenol, and intermolecular hydrogen bonding. Analysis of FTIR shows that the C=C and C=N groups contribute to phenol adsorption onto the *[poly(EGDMA-VIM)]* microspheres' surfaces.

According to Fig. 7b, the structures of the polymer microspheres did not change after phenol adsorption. However, some small alterations in peak intensity due to changes in the network parameters were shown in the XRD

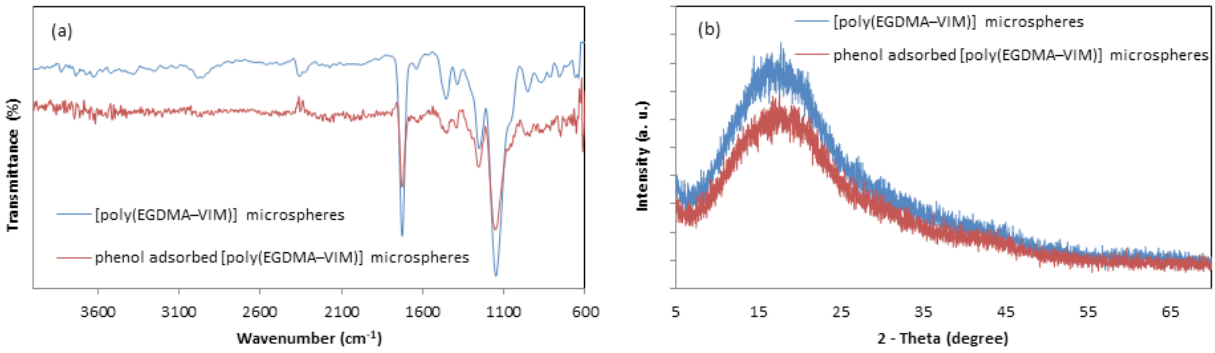

Fig. 7 (a) FTIR spectrum (b) XRD patterns for the *[poly(EGDMA–VIM)]* microspheres before and after adsorption of phenol.

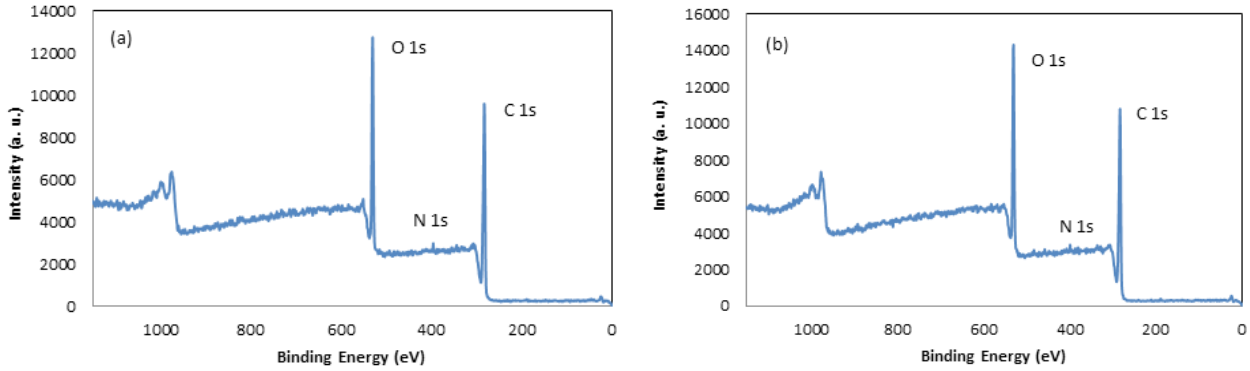

Fig. 8. XPS energy spectra of the *[poly(EGDMA–VIM)]* microspheres (a) before and (b) after phenol adsorption.

pattern of the phenol adsorbed on the *[poly(EGDMA-VIM)]* microspheres.

According to Figs. 8a and 8b, the peaks of C 1s and O 1s were enhanced for the *[poly(EGDMA-VIM)]* microspheres' surfaces treated with phenol whereas the peaks of N 1s were weakened. From the results of XPS analysis, the contents of C 1s, O 1s, and N 1s were 70.2%, 29.1%, and 0.7% on the polymer microspheres' surfaces before adsorption and 70.4%, 29.4% and 0.2% on the *[poly(EGDMA-VIM)]* microspheres' surfaces after adsorption, respectively. The contents of C 1s and O 1s increased but the contents of O 1s decreased after phenol adsorption. The adsorption of phenol makes the *[poly(EGDMA-VIM)]* microspheres' surfaces much more hydrophobic due to the increased C content at the polymer microspheres' surfaces [61] because they are significantly covered by phenol. The decrease in the content and increase in binding energy (from 399.5 to 400.3) of N 1s mainly results from the H-bond between the –OH group of phenol and nitrogen atoms in the vinylimidazole of the *[poly(EGDMA-VIM)]* microspheres.

Additionally, at pH values of 3.95 to 9, the surfaces of the polymer microspheres are negatively charged, so an electrostatic mechanism cannot explain the experimental finding. The intermolecular hydrogen bond (OH· · ·N) between the nitrogen atoms in the vinylimidazole of the *[poly(EGDMA-VIM)]* microspheres and the phenolic hydroxyl group at pH < pKa, is favorable for adsorption. According to the XPS, FTIR, XRD, Zeta-potential and pH experiments, the possible interactions between phenol and the polymeric chain are shown in Fig. 9.

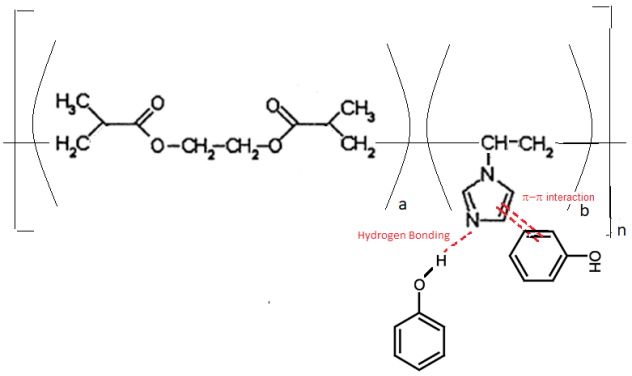

Fig. 9. Possible interactions between the *[poly(EGDMA–VIM)]* microspheres and the phenol.

4. Conclusions

In the present study, the *[poly(EGDMA-VIM)]* microspheres with high surface area (304.4 $m^2 g^{-1}$)were prepared by the suspension polymerization method, and characterized and used as an adsorbent for phenol removal. The results indicated that the phenol-removal capacity of the *[poly(EGDMA-VIM)]* microspheres increased when the initial concentration of phenol solutions was increased and decreased when the pH and temperature increased. It was found that the Freundlich isotherm and pseudo-second-order kinetic models could accurately describe the phenol adsorption onto the *[poly(EGDMA-VIM)]* microspheres.

The results of adsorption thermodynamics revealed that the phenol adsorption was a spontaneous and exothermic process. The *[poly(EGDMA-VIM)]* microspheres possessed suitable reusability properties. The adsorption mechanism can be explained by the fact that the hydrogen bond between the nitrogen atoms in the vinylimidazole segment of the *[poly(EGDMA-VIM)]* microspheres and the hydroxyl groups of phenol play an important role in the adsorption process.

Acknowledgement

This work was supported by the Scientific and Technological Research Council of Turkey, TÜBİTAK under Project Number 117Y271. We would like to thank TÜBİTAK for its financial support.

References

[1] C. Păcurariu, G. Mihoc, A. Popa, S.G. Muntean, R. Ianoş, Adsorption of phenol and p-chlorophenol from aqueous solutions on poly (styrene-co-divinylbenzene) functionalized materials, Chem. Eng. J., 222 (2013) 218–227.
[2] O. Abdelwahab, N.K. Amin, E.-S.Z. El-Ashtoukhy, The investigation of phenol removal from aqueous solutions by water hyacinth, Sep. Sci. Technol., 49 (2014) 1604–1612.
[3] V.K. Gupta, M. Sharma, K. Singh, R.K. Vyas, Reactive adsorption of phenol onto Fe-GAC: Parallel pore batch modeling and experimental studies, J. Taiwan Inst. Chem. Eng., 63 (2016) 116–124.
[4] J. Yin, R. Chen, Y. Ji, C. Zhao, G. Zhao, H. Zhang, Adsorption of phenols by magnetic polysulfone microcapsules containing tributyl phosphate, Chem. Eng. J., 157 (2010) 466–474.
[5] F. Moradi, M.D. Ganji, Y. Sarrafi, Remediation of phenol-contaminated water by pristine and functionalized SWCNTs: Ab initio van der Waals DFT investigation, Diam. Relat. Mater., 82 (2018) 7–18.
[6] Z.M. Ahmed, S. Lyne, R. Shahrabani, Removal and recovery of phenol from phenolic wastewater via ion exchange and polymeric resins, Environ. Eng. Sci., 17 (2000) 245–255.
[7] Y. Tai, L. Wang, J. Gao, W.A. Amer, W. Ding, H. Yu, Synthesis of Fe_3O_4@poly(methylmethacrylate-co-divinylbenzene) magnetic porous microspheres and their application in the separation of phenol from aqueous solutions, J. Colloid Interf. Sci., 360 (2011) 731–738.
[8] W. Cichy, J. Szymanowski, Recovery of phenol from aqueous streams in hollowfiber modules, Environ. Sci. Technol., 36 (2002) 2088–2093.
[9] Z. Li, M. Wu, Z. Jiao, B. Bao, S. Lu, Extraction of phenol from wastewater by N-octonoylpyrrolidine, J. Hazard. Mater. B, 114 (2004) 111–114.
[10] L.Z. Wang, Y.M. Zhao, J.F. Fu, The influence of TiO_2 and aeration on the kinetics of electrochemical oxidation of phenol in packed bed reactor, J. Hazard. Mater., 160 (2008) 608–613.
[11] H.B. Senturk, D. Ozdes, A. Gundogdu, C. Duran, M. Soylak, Removal of phenol from aqueous solutions by adsorption onto organomodified Tirebolu bentonite: equilibrium, kinetic and thermodynamic study, J. Hazard. Mater., 172 (2009) 353–362.
[12] K. Baransi, Y. Dubowski, I. Sabbah, Synergetic effect between photocatalytic degradation and adsorption processes on the removal of phenolic compounds from olive mill wastewater, Water Res., 46 (2012) 789–798.
[13] D. Peredo-Mancilla, H. Dominguez, Adsorption of phenol molecules by sodium dodecyl sulfate (SDS) surfactants deposited on solid surfaces: A computer simulation study, J. Mol. Graph. Model., 65 (2016) 108–112.
[14] F.A. Banat, B. Al-Bashir, S. Al-Asheh, O. Hayajneh, Adsorption of phenol by bentonite, Environ. Pollut., 107 (2000) 391–398.
[15] A.Y. Cetinkaya, O.K. Ozdemir, Phenol removal from synthetic solution using low pressure membranes coated with graphene oxide and carbon, Chem. Pap., 72 (2018) 327–335.
[16] B.C. Pan, W. Du, W.M. Zhang, X. Zhang, Q.R. Zhang, B.J. Pan, L. Lv, Q.X. Zhang, J.L. Chen, Improved adsorption of 4-nitrophenol onto a novel hyper-cross-linked polymer, Environ. Sci. Technol., 41 (2007) 5057–5062.
[17] K.M. Smith, G.D. Fowler, S. Pullket, N.J.D. Graham, Sewage sludge-based adsorbents: a review of their production, properties and use in water treatment applications, Water Res., 43 (2009) 2569–2594.
[18] L. Damjanovic, V. Rakic, V. Rac, D. Stosic, A. Auroux, The investigation of phenol removal from aqueous solutions by zeolites as solid adsorbents, J. Hazard. Mater., 184 (2010) 477–484.
[19] Ihsanullah, H.A. Asmaly, T.A. Saleh, T. Laoui, V.K. Gupta, M.A. Atieh, Enhanced adsorption of phenols from liquids by aluminum oxide/carbon nanotubes: Comprehensive study from synthesis to surface properties, J. Mol. Liq., 206 (2015) 176–182.
[20] B. Abussaud, H.A. Asmaly, Ihsanullah, T.A. Saleh, V.K. Gupta, T. Laoui, M.A. Atieh, Sorption of phenol from waters on activated carbon impregnated with iron oxide, aluminum oxide and titanium oxide, J. Mol. Liq., 213 (2016) 351–359.
[21] Y. Li, X. Hu, X. Liu, Y. Zhang, Q. Zhao, P. Ning, S. Tian, Adsorption behavior of phenol by reversible surfactant-modified montmorillonite: Mechanism, thermodynamics, and regeneration, Chem. Eng. J., 334 (2018) 1214–1221.
[22] A. Denizli, G. Özkan, M. Uçar, Removal of chlorophenols from aquatic systems with dye-affinity microbeads, Sep. Purif. Technol., 24 (2001) 255–262.
[23] İ. Abay, A. Denizli, E. Bişkin, B. Salih, Removal and pre-concentration of phenolic species onto β-cyclodextrin modified poly(hydroxyethylmethacrylate-ethyleneglycoldimethacrylate) microbeads, Chemosphere, 61 (2005) 1263–1272.
[24] N. Kawabata, Y. Tsuchida, Y. Nakamori, M. Kitamura, Adsorption of phenol on clustered micro-sphere porous beads made of cross-linked poly-4-vinylpyridine, React. Funct. Polym., 66 (2006) 1641–1648.
[25] S.K. Nadavala, K. Swayampakula, V.M. Boddu, K. Abburi, Biosorption of phenol and *o*-chlorophenol from aqueous solutions on to chitosan-calcium alginate blended beads, J. Hazard. Mater., 162 (2009) 482–489.
[26] F. Belaib, A.H. Meniai, M.B. Lehocine, Elimination of phenol by adsorption onto mineral/polyaniline composite solid support, Energy Procedia., 18 (2012) 1254–1260.
[27] S. Yuan, J. Gu, Y. Zheng, W. Jiang, B. Liang, S.O. Pehkonen, Purification of phenol-contaminated water by adsorption with quaternized poly(dimethylaminopropyl methacrylamide)-grafted PVBC microspheres, J. Mater. Chem. A, 3 (2015) 4620–4636.
[28] M.L. Nguyen, C. Huang, R.-S. Juang, Synergistic biosorption between phenol and nickel(II) from binary mixtures on chemically and biologically modified chitosan beads, Chem. Eng. J., 286 (2016) 68–75.
[29] G. Xiao, R. Wen, P. You, D. Wu, Adsorption of phenol onto four hyper-cross-linked polymeric adsorbents: Effect of hydrogen bonding receptor in micropores on adsorption capacity, Micropor. Mesopor. Mat., 239 (2017) 40–44.
[30] J.A. Galicia-Aguilar, J.D. Santamaría-Juárez, M. López-Badillo, M. Sánchez-Cantú, J.L. Varela-Caselis, Synthesis and characterization of AN/EGDMA-based adsorbents for phenol Adsorption, React. Funct. Polym., 117 (2017) 112–119.
[31] A. Kara, S. Aksoy, N. Beşirli, Adsorption properties of Cr(VI) onto microspheres carrying imidazole functional groups: kinetic and isotherm studies, Hacettepe J. Biol. Chem., 40 (2012) 37–44.

[32] A. Kara, L. Uzun, N. Beşirli, A. Denizli, Poly(ethylene glycol dimethacrylate-*n*-vinyl imidazole) beads for heavy metal removal, J. Hazard. Mater., 106B (2004) 93–99.
[33] B. Osman, A. Kara, N. Beşirli, Tyrosinase immobilization on Cu^{2+} chelated Poly(ethylene glycol dimethacrylate-N-Vinyl Imidazole) beads, Hacettepe J. Biol. Chem., 35 (2007) 233–241.
[34] B. Osman, A. Kara, L. Uzun, N. Beşirli, A. Denizli, Vinyl imidazole carrying metal-chelated beads for reversible use in yeast invertase adsorption, J. Mol. Catal. B-Enzym., 37 (2005) 88–94.
[35] A. Kara, B. Osman, H. Yavuz, N. Beşirli, A. Denizli, Immobilization of α-amylase on Cu^{2+} chelated poly(ethylene glycol dimethacrylate-n-vinyl imidazole) matrix via adsorption, React. Funct. Polym., 62 (2005) 61–68.
[36] M.G. Segatelli, V.S. Santos, A.B.T. Presotto, I.V.P. Yoshida, C.R.T. Tarley, Cadmium ion-selective sorbent preconcentration method using ion imprinted poly(ethylene glycol dimethacrylate-co-vinylimidazole), React. Funct. Polym., 70 (2010) 325–333.
[37] C.R.T. Tarley, M.Z. Corazza, B.F. Somera, M.G. Segatelli, Preparation of new ion-selective cross-linked poly(vinylimidazole-*co*-ethyleneglycol dimethacrylate) using a double-imprinting process for the preconcentration of Pb^{2+} ions, J. Colloid Interf. Sci., 450 (2015) 254–263.
[38] D. Schemeth, C. Kappacher, M. Rainer, R. Thalinger, G.K. Bonn, Comprehensive evaluation of imidazole-based polymers for the enrichment of selected non-steroidal anti-inflammatory drugs, Talanta, 153 (2016) 177–185.
[39] D. Schemeth, J.C. Noël, T. Jakschitz, M. Rainer, R. Tessadri, C.W. Huck, G.K. Bonn, Poly(N-vinylimidazole/ethylene glycol dimethacrylate) for the purification and isolation of phenolic acids, Anal. Chim. Acta, 885 (2015) 199–206.
[40] E. Uğuzdoğan, E.B. Denkbaş, E. Öztürk, S.A. Tuncel, O.S. Kabasakal, Preparation and characterization of polyethyleneglycolmethacrylate(PEGMA)-*co*-vinylimidazole (VI) microspheres to use in heavy metal removal, J. Hazard. Mater., 162 (2009) 1073–1080.
[41] E. Uğuzdoğan, E.B. Denkbaş, O.S. Kabasakal, The use of polyethyleneglycolmethacrylate-*co*-vinylimidazole (PEGMA-*co*-VI) microspheres for the removal of nickel(II) and chromium(VI) ions, J. Hazard. Mater., 177 (2010) 119–125.
[42] S. Senel, L. Uzun, A. Kara, A. Denizli, Heavy metal removal from synthetic solutions with magnetic beads under magnetic field, J.Macromol. Sci. A, 45 (2008) 635–642.
[43] Z. Guan, L. Liu, L. He, S. Yang, Amphiphilic hollow carbonaceous microspheres for the sorption of phenol from Water, J. Hazard. Mater., 196 (2011) 270–277.
[44] K.K. Jaiswal, D. Manikandan, R. Murugan, A.P. Ramaswamy, Microwave-assisted rapid synthesis of Fe_3O_4/poly(styrene-divinylbenzeneacrylic acid) polymeric magnetic composites and investigation of their structural and magnetic properties, Eur. Polym. J., 98 (2018) 177–190.
[45] X. Gao, Y. Dai, Y. Zhang, F. Fu, Effective adsorption of phenolic compound from aqueous solutions on activated semi coke, J. Phys. Chem. Solids, 102 (2017) 142–150.
[46] J. Li, Q. Zhou, Y. Wu, Y. Yuan, Y. Liu, Investigation of nanoscale zerovalent iron-based magnetic and thermal dual-responsive composite materials for the removal and detection of phenols, Chemosphere, 195 (2018) 472–482.
[47] X. Wang, H. Ou, J. Huang, One-pot synthesis of hyper-crosslinked polymers chemically modified with pyrrole, furan, and thiophene for phenol adsorption from aqueous solution, J. Colloid Interf. Sci., 538 (2019) 499–506.
[48] D. Zhang, P. Huo, W. Liu, Behavior of phenol adsorption on thermal modified activated carbon, Chinese J. Chem. Eng., 24 (2016) 446–452.
[49] X. Qiu, N. Li, X. Ma, S. Yang, Q. Xu, H. Li, J. Lu, Facile preparation of acrylic ester-based crosslinked resin and its adsorption of phenol at high concentration, J. Environ. Chem. Eng., 2 (2014) 745–751.
[50] W.P. Cheng, W. Gao, X. Cui, J.H. Ma, R.F. Li, Phenol adsorption equilibrium and kinetics on zeolite X/activated carbon composite, J. Taiwan Inst. Chem. E., 62 (2016) 192–198.
[51] E.T. Özer, B. Osman, A. Kara, N. Beşirli, Ş. Gücer, H. Sözeri, Removal of diethyl phthalate from aqueous phase using magnetic poly(EGDMA-VP) beads, J. Hazard. Mater., 229–230 (2012) 20–28. https://doi.org/10.1016/j.jhazmat.2012.05.037.
[52] J. Feng, H. Ding, G. Yang, R. Wang, S. Li, J. Liao, Z. Li, D. Chen, Preparation of black-pearl reduced graphene oxide–sodium alginate hydrogel microspheres for adsorbing organic pollutants, J. Colloid Interf. Sci., 508 (2017) 387–395.
[53] J. Sun, X. Liu, F. Zhang, J. Zhou, J. Wu, A. Alsaedi, T. Hayat, J. Li, Insight into the mechanism of adsorption of phenol and resorcinol on activated carbons with different oxidation degrees, Colloid. Surface A, 563 (2019) 22–30.
[54] A. Kara, E. Demirbel, N. Tekin, B. Osman, N. Beşirli, Magnetic vinylphenylboronic acid microparticles for Cr(VI) adsorption: Kinetic, isotherm and thermodynamic studies, J. Hazard. Mater., 286 (2015) 612–623.
[55] A. Adak, A. Pal, M. Bandyopadhyay, Removal of phenol from water environment by surfactant-modified alumina through adsolubilization, Colloids Surf. A: Physicochem. Eng. Asp., 277 (2006) 63–68.
[56] Z. Gong, S. Li, W. Han, J. Wang, J. Ma, X. Zhang, Recyclable graphene oxide grafted with poly(N-isopropylacrylamide) and its enhanced selective adsorption for phenols, Appl. Surf. Sci., 362 (2016) 459–468.
[57] J. Han, Z. Du, W. Zou, H. Li, C. Zhang, In-situ improved phenol adsorption at ions-enrichment interface of porous adsorbent for simultaneous removal of copper ions and phenol, Chem. Eng. J., 262 (2015) 571–578.
[58] A.H. Al-Muhtaseb, K.A. Ibrahim, A.B. Albadarin, O. Ali-khashman, G.M. Walker, M.N.M. Ahmad, Remediation of phenol-contaminated water by adsorption using poly(methyl methacrylate) (PMMA), Chem. Eng. J., 168 (2011) 691–699.
[59] B.N. Bhadra, I. Ahmed, S.H. Jhung, Remarkable adsorbent for phenol removal from fuel: Functionalized metal-organic framework, Fuel, 174 (2016) 43–48.
[60] L. Lupa, L. Cocheci, R. Pode, I. Hulka, Phenol adsorption using Aliquat 336 functionalized Zn-Al layered double hydroxide, Sep. Purif. Technol., 196 (2018) 82–95.
[61] X. Lyu, X. You, M. He, W. Zhang, H. Wei, L. Li, Q. He, Adsorption and molecular dynamics simulations of nonionic surfactant on the low rank coal surface, Fuel, 211 (2018) 529–534.